

Measurement of the $t\bar{t}$ production cross section in $p\bar{p}$ collisions at $\sqrt{s} = 1.96$ TeV

V.M. Abazov³⁶, B. Abbott⁷⁵, M. Abolins⁶⁵, B.S. Acharya²⁹, M. Adams⁵¹, T. Adams⁴⁹, E. Aguilo⁶, S.H. Ahn³¹, M. Ahsan⁵⁹, G.D. Alexeev³⁶, G. Alkhazov⁴⁰, A. Alton^{64,a}, G. Alverson⁶³, G.A. Alves², M. Anastasoie³⁵, L.S. Ancu³⁵, T. Andeen⁵³, S. Anderson⁴⁵, B. Andrieu¹⁷, M.S. Anzelc⁵³, M. Aoki⁵⁰, Y. Arnoud¹⁴, M. Arov⁶⁰, M. Arthaud¹⁸, A. Askew⁴⁹, B. Åsman⁴¹, A.C.S. Assis Jesus³, O. Atramentov⁴⁹, C. Avila⁸, C. Ay²⁴, F. Badaud¹³, A. Baden⁶¹, L. Bagby⁵⁰, B. Baldin⁵⁰, D.V. Bandurin⁵⁹, P. Banerjee²⁹, S. Banerjee²⁹, E. Barberis⁶³, A.-F. Barfuss¹⁵, P. Bargassa⁸⁰, P. Baringer⁵⁸, J. Barreto², J.F. Bartlett⁵⁰, U. Bassler¹⁸, D. Bauer⁴³, S. Beale⁶, A. Bean⁵⁸, M. Begalli³, M. Begel⁷³, C. Belanger-Champagne⁴¹, L. Bellantoni⁵⁰, A. Bellavance⁵⁰, J.A. Benitez⁶⁵, S.B. Beri²⁷, G. Bernardi¹⁷, R. Bernhard²³, I. Bertram⁴², M. Besançon¹⁸, R. Beuselinck⁴³, V.A. Bezzubov³⁹, P.C. Bhat⁵⁰, V. Bhatnagar²⁷, C. Biscarat²⁰, G. Blazey⁵², F. Blekman⁴³, S. Blessing⁴⁹, D. Bloch¹⁹, K. Bloom⁶⁷, A. Boehnlein⁵⁰, D. Boline⁶², T.A. Bolton⁵⁹, G. Borisso⁴², T. Bose⁷⁷, A. Brandt⁷⁸, R. Brock⁶⁵, G. Brooijmans⁷⁰, A. Bross⁵⁰, D. Brown⁸¹, N.J. Buchanan⁴⁹, D. Buchholz⁵³, M. Buehler⁸¹, V. Buescher²², V. Bunichev³⁸, S. Burdin^{42,b}, S. Burke⁴⁵, T.H. Burnett⁸², C.P. Buszello⁴³, J.M. Butler⁶², P. Calfayan²⁵, S. Calvet¹⁶, J. Cammin⁷¹, W. Carvalho³, B.C.K. Casey⁵⁰, H. Castilla-Valdez³³, S. Chakrabarti¹⁸, D. Chakraborty⁵², K. Chan⁶, K.M. Chan⁵⁵, A. Chandra⁴⁸, F. Charles^{19,‡}, E. Cheu⁴⁵, F. Chevallier¹⁴, D.K. Cho⁶², S. Choi³², B. Choudhary²⁸, L. Christofek⁷⁷, T. Christoudias⁴³, S. Cihangir⁵⁰, D. Claes⁶⁷, Y. Coadou⁶, M. Cooke⁸⁰, W.E. Cooper⁵⁰, M. Corcoran⁸⁰, F. Couderc¹⁸, M.-C. Cousinou¹⁵, S. Crépe-Renaudin¹⁴, D. Cutts⁷⁷, M. Œwiok³⁰, H. da Motta², A. Das⁴⁵, G. Davies⁴³, K. De⁷⁸, S.J. de Jong³⁵, E. De La Cruz-Burelo⁶⁴, C. De Oliveira Martins³, J.D. Degenhardt⁶⁴, F. Déliot¹⁸, M. Demarteau⁵⁰, R. Demina⁷¹, D. Denisov⁵⁰, S.P. Denisov³⁹, S. Desai⁵⁰, H.T. Diehl⁵⁰, M. Diesburg⁶⁷, A. Dominguez⁶⁷, H. Dong⁷², L.V. Dudko³⁸, L. Duflot¹⁶, S.R. Dugad²⁹, D. Duggan⁴⁹, A. Duperrin¹⁵, J. Dyer⁶⁵, A. Dyshkant⁵², M. Eads⁶⁷, D. Edmunds⁶⁵, J. Ellison⁴⁸, V.D. Elvira⁵⁰, Y. Enari⁷⁷, S. Eno⁶¹, P. Ermolov³⁸, H. Evans⁵⁴, A. Evdokimov⁷³, V.N. Evdokimov³⁹, A.V. Ferapontov⁵⁹, T. Ferbel⁷¹, F. Fiedler²⁴, F. Filthaut³⁵, W. Fisher⁵⁰, H.E. Fisk⁵⁰, M. Fortner⁵², H. Fox⁴², S. Fu⁵⁰, S. Fuess⁵⁰, T. Gadfort⁷⁰, C.F. Galea³⁵, E. Gallas⁵⁰, C. Garcia⁷¹, A. Garcia-Bellido⁸², V. Gavrilov³⁷, P. Gay¹³, W. Geist¹⁹, D. Gelé¹⁹, C.E. Gerber⁵¹, Y. Gershtein⁴⁹, D. Gillberg⁶, G. Ginther⁷¹, N. Gollub⁴¹, B. Gómez⁸, A. Goussiou⁸², P.D. Grannis⁷², H. Greenlee⁵⁰, Z.D. Greenwood⁶⁰, E.M. Gregores⁴, G. Grenier²⁰, Ph. Gris¹³, J.-F. Grivaz¹⁶, A. Grohsjean²⁵, S. Grünendahl⁵⁰, M.W. Grünewald³⁰, F. Guo⁷², J. Guo⁷², G. Gutierrez⁵⁰, P. Gutierrez⁷⁵, A. Haas⁷⁰, N.J. Hadley⁶¹, P. Haefner²⁵, S. Hagopian⁴⁹, J. Haley⁶⁸, I. Hall⁶⁵, R.E. Hall⁴⁷, L. Han⁷, K. Harder⁴⁴, A. Harel⁷¹, R. Harrington⁶³, J.M. Hauptman⁵⁷, R. Hauser⁶⁵, J. Hays⁴³, T. Hebbeker²¹, D. Hedin⁵², J.G. Hegeman³⁴, J.M. Heinmiller⁵¹, A.P. Heinson⁴⁸, U. Heintz⁶², C. Hensel⁵⁸, K. Herner⁷², G. Hesketh⁶³, M.D. Hildreth⁵⁵, R. Hirosky⁸¹, J.D. Hobbs⁷², B. Hoeneisen¹², H. Hoeth²⁶, M. Hohlfeld²², S.J. Hong³¹, S. Hossain⁷⁵, P. Houben³⁴, Y. Hu⁷², Z. Hubacek¹⁰, V. Hynek⁹, I. Iashvili⁶⁹, R. Illingworth⁵⁰, A.S. Ito⁵⁰, S. Jabeen⁶², M. Jaffré¹⁶, S. Jain⁷⁵, K. Jakobs²³, C. Jarvis⁶¹, R. Jesik⁴³, K. Johns⁴⁵, C. Johnson⁷⁰, M. Johnson⁵⁰, A. Jonckheere⁵⁰, P. Jonsson⁴³, A. Juste⁵⁰, E. Kajfasz¹⁵, A.M. Kalinin³⁶, J.M. Kalk⁶⁰, S. Kappler²¹, D. Karmanov³⁸, P.A. Kasper⁵⁰, I. Katsanos⁷⁰, D. Kau⁴⁹, V. Kaushik⁷⁸, R. Kehoe⁷⁹, S. Kermiche¹⁵, N. Khalatyan⁵⁰, A. Khanov⁷⁶, A. Kharchilava⁶⁹, Y.M. Kharzheev³⁶, D. Khatidze⁷⁰, T.J. Kim³¹, M.H. Kirby⁵³, M. Kirsch²¹, B. Klima⁵⁰, J.M. Kohli²⁷, J.-P. Konrath²³, V.M. Korablev³⁹, A.V. Kozelov³⁹, J. Kraus⁶⁵, D. Krop⁵⁴, T. Kuhl²⁴, A. Kumar⁶⁹, A. Kupco¹¹, T. Kurča²⁰, J. Kvita⁹, F. Lacroix¹³, D. Lam⁵⁵, S. Lammers⁷⁰, G. Landsberg⁷⁷, P. Lebrun²⁰, W.M. Lee⁵⁰, A. Leflat³⁸, J. Lellouch¹⁷, J. Leveque⁴⁵, J. Li⁷⁸, L. Li⁴⁸, Q.Z. Li⁵⁰, S.M. Lietti⁵, J.G.R. Lima⁵², D. Lincoln⁵⁰, J. Linnemann⁶⁵, V.V. Lipaev³⁹, R. Lipton⁵⁰, Y. Liu⁷, Z. Liu⁶, A. Lobodenko⁴⁰, M. Lokajicek¹¹, P. Love⁴², H.J. Lubatti⁸², R. Luna³, A.L. Lyon⁵⁰, A.K.A. Maciel², D. Mackin⁸⁰, R.J. Madaras⁴⁶, P. Mättig²⁶, C. Magass²¹, A. Magerkurth⁶⁴, P.K. Mal⁸², H.B. Malbouisson³, S. Malik⁶⁷, V.L. Malyshev³⁶, H.S. Mao⁵⁰, Y. Maravin⁵⁹, B. Martin¹⁴, R. McCarthy⁷², A. Melnitchouk⁶⁶, L. Mendoza⁸, P.G. Mercadante⁵, M. Merkin³⁸, K.W. Merritt⁵⁰, A. Meyer²¹, J. Meyer^{22,d}, T. Millet²⁰, J. Mitrevski⁷⁰, J. Molina³, R.K. Mommsen⁴⁴, N.K. Mondal²⁹, R.W. Moore⁶, T. Moulik⁵⁸, G.S. Muanza²⁰, M. Mulders⁵⁰, M. Mulhearn⁷⁰, O. Mundal²², L. Mundim³, E. Nagy¹⁵, M. Naimuddin⁵⁰, M. Narain⁷⁷, N.A. Naumann³⁵, H.A. Neal⁶⁴, J.P. Negret⁸, P. Neustroev⁴⁰, H. Nilsen²³, H. Nogima³, S.F. Novaes⁵, T. Nunnemann²⁵, V. O'Dell⁵⁰, D.C. O'Neil⁶, G. Obrant⁴⁰, C. Ochando¹⁶, D. Onoprienko⁵⁹, N. Oshima⁵⁰, N. Osman⁴³, J. Osta⁵⁵, R. Otec¹⁰, G.J. Otero y Garzón⁵⁰, M. Owen⁴⁴, P. Padley⁸⁰, M. Pangilinan⁷⁷, N. Parashar⁵⁶, S.-J. Park⁷¹, S.K. Park³¹, J. Parsons⁷⁰, R. Partridge⁷⁷, N. Parua⁵⁴, A. Patwa⁷³, G. Pawloski⁸⁰, B. Penning²³, M. Perfilov³⁸, K. Peters⁴⁴,

Y. Peters²⁶, P. Pétroff¹⁶, M. Petteni⁴³, R. Piegai¹, J. Piper⁶⁵, M.-A. Pleier²², P.L.M. Podesta-Lerma^{33,c},
V.M. Podstavkov⁵⁰, Y. Pogorelov⁵⁵, M.-E. Pol², P. Polozov³⁷, B.G. Pope⁶⁵, A.V. Popov³⁹, C. Potter⁶,
W.L. Prado da Silva³, H.B. Prosper⁴⁹, S. Protopopescu⁷³, J. Qian⁶⁴, A. Quadt^{22,d}, B. Quinn⁶⁶, A. Rakitine⁴²,
M.S. Rangel², K. Ranjan²⁸, P.N. Ratoff⁴², P. Renkel⁷⁹, S. Reucroft⁶³, P. Rich⁴⁴, J. Rieger⁵⁴, M. Rijssenbeek⁷²,
I. Ripp-Baudot¹⁹, F. Rizatdinova⁷⁶, S. Robinson⁴³, R.F. Rodrigues³, M. Rominsky⁷⁵, C. Royon¹⁸, P. Rubinov⁵⁰,
R. Ruchti⁵⁵, G. Safronov³⁷, G. Sajot¹⁴, A. Sánchez-Hernández³³, M.P. Sanders¹⁷, A. Santoro³, G. Savage⁵⁰,
L. Sawyer⁶⁰, T. Scanlon⁴³, D. Schaile²⁵, R.D. Schamberger⁷², Y. Scheglov⁴⁰, H. Schellman⁵³, T. Schliephake²⁶,
C. Schwanenberger⁴⁴, A. Schwartzman⁶⁸, R. Schwienhorst⁶⁵, J. Sekaric⁴⁹, H. Severini⁷⁵, E. Shabalina⁵¹,
M. Shamim⁵⁹, V. Shary¹⁸, A.A. Shchukin³⁹, R.K. Shivpuri²⁸, V. Siccaldi¹⁹, V. Simak¹⁰, V. Sirotenko⁵⁰, P. Skubic⁷⁵,
P. Slattery⁷¹, D. Smirnov⁵⁵, G.R. Snow⁶⁷, J. Snow⁷⁴, S. Snyder⁷³, S. Söldner-Rembold⁴⁴, L. Sonnenschein¹⁷,
A. Sopczak⁴², M. Sosebee⁷⁸, K. Soustruznik⁹, B. Spurlock⁷⁸, J. Stark¹⁴, J. Steele⁶⁰, V. Stolin³⁷, D.A. Stoyanova³⁹,
J. Strandberg⁶⁴, S. Strandberg⁴¹, M.A. Strang⁶⁹, E. Strauss⁷², M. Strauss⁷⁵, R. Ströhmer²⁵, D. Strom⁵³,
L. Stutte⁵⁰, S. Sumowidagdo⁴⁹, P. Svoisky⁵⁵, A. Sznajder³, P. Tamburello⁴⁵, A. Tanasijczuk¹, W. Taylor⁶,
J. Temple⁴⁵, B. Tiller²⁵, F. Tissandier¹³, M. Titov¹⁸, V.V. Tokmenin³⁶, T. Toole⁶¹, I. Torchiani²³, T. Trefzger²⁴,
D. Tsybychev⁷², B. Tuchming¹⁸, C. Tully⁶⁸, P.M. Tuts⁷⁰, R. Unalan⁶⁵, L. Uvarov⁴⁰, S. Uvarov⁴⁰, S. Uzunyan⁵²,
B. Vachon⁶, P.J. van den Berg³⁴, R. Van Kooten⁵⁴, W.M. van Leeuwen³⁴, N. Varelas⁵¹, E.W. Varnes⁴⁵,
I.A. Vasilyev³⁹, M. Vaupel²⁶, P. Verdier²⁰, L.S. Vertogradov³⁶, M. Verzocchi⁵⁰, F. Villeneuve-Segui⁴³, P. Vint⁴³,
P. Vokac¹⁰, E. Von Toerne⁵⁹, M. Voutilainen^{68,e}, R. Wagner⁶⁸, H.D. Wahl⁴⁹, L. Wang⁶¹, M.H.L.S. Wang⁵⁰,
J. Warchol⁵⁵, G. Watts⁸², M. Wayne⁵⁵, G. Weber²⁴, M. Weber⁵⁰, L. Welty-Rieger⁵⁴, A. Wenger^{23,f},
N. Worms²², M. Wetstein⁶¹, A. White⁷⁸, D. Wicke²⁶, G.W. Wilson⁵⁸, S.J. Wimpenny⁴⁸, M. Wobisch⁶⁰,
D.R. Wood⁶³, T.R. Wyatt⁴⁴, Y. Xie⁷⁷, S. Yacoub⁵³, R. Yamada⁵⁰, M. Yan⁶¹, T. Yasuda⁵⁰, Y.A. Yatsunen³⁶,
K. Yip⁷³, H.D. Yoo⁷⁷, S.W. Youn⁵³, J. Yu⁷⁸, A. Zatserklyaniy⁵², C. Zeitnitz²⁶, T. Zhao⁸², B. Zhou⁶⁴,
J. Zhu⁷², M. Zielinski⁷¹, D. Zieminska⁵⁴, A. Zieminski^{54,‡}, L. Zivkovic⁷⁰, V. Zutshi⁵², and E.G. Zverev³⁸

(The DØ Collaboration)

¹Universidad de Buenos Aires, Buenos Aires, Argentina

²LAFEX, Centro Brasileiro de Pesquisas Físicas, Rio de Janeiro, Brazil

³Universidade do Estado do Rio de Janeiro, Rio de Janeiro, Brazil

⁴Universidade Federal do ABC, Santo André, Brazil

⁵Instituto de Física Teórica, Universidade Estadual Paulista, São Paulo, Brazil

⁶University of Alberta, Edmonton, Alberta, Canada,

Simon Fraser University, Burnaby, British Columbia,

Canada, York University, Toronto, Ontario, Canada,

and McGill University, Montreal, Quebec, Canada

⁷University of Science and Technology of China, Hefei, People's Republic of China

⁸Universidad de los Andes, Bogotá, Colombia

⁹Center for Particle Physics, Charles University, Prague, Czech Republic

¹⁰Czech Technical University, Prague, Czech Republic

¹¹Center for Particle Physics, Institute of Physics,

Academy of Sciences of the Czech Republic, Prague, Czech Republic

¹²Universidad San Francisco de Quito, Quito, Ecuador

¹³LPC, Univ Blaise Pascal, CNRS/IN2P3, Clermont, France

¹⁴LPSC, Université Joseph Fourier Grenoble 1, CNRS/IN2P3,

Institut National Polytechnique de Grenoble, France

¹⁵CPPM, IN2P3/CNRS, Université de la Méditerranée, Marseille, France

¹⁶LAL, Univ Paris-Sud, IN2P3/CNRS, Orsay, France

¹⁷LPNHE, IN2P3/CNRS, Universités Paris VI and VII, Paris, France

¹⁸DAPNIA/Service de Physique des Particules, CEA, Saclay, France

¹⁹IPHC, Université Louis Pasteur et Université de Haute Alsace, CNRS/IN2P3, Strasbourg, France

²⁰IPNL, Université Lyon 1, CNRS/IN2P3, Villeurbanne, France and Université de Lyon, Lyon, France

²¹III. Physikalisches Institut A, RWTH Aachen, Aachen, Germany

²²Physikalisches Institut, Universität Bonn, Bonn, Germany

²³Physikalisches Institut, Universität Freiburg, Freiburg, Germany

²⁴Institut für Physik, Universität Mainz, Mainz, Germany

²⁵Ludwig-Maximilians-Universität München, München, Germany

²⁶Fachbereich Physik, University of Wuppertal, Wuppertal, Germany

²⁷Panjab University, Chandigarh, India

²⁸Delhi University, Delhi, India

- ²⁹Tata Institute of Fundamental Research, Mumbai, India
³⁰University College Dublin, Dublin, Ireland
³¹Korea Detector Laboratory, Korea University, Seoul, Korea
³²SungKyunKwan University, Suwon, Korea
³³CINVESTAV, Mexico City, Mexico
³⁴FOM-Institute NIKHEF and University of Amsterdam/NIKHEF, Amsterdam, The Netherlands
³⁵Radboud University Nijmegen/NIKHEF, Nijmegen, The Netherlands
³⁶Joint Institute for Nuclear Research, Dubna, Russia
³⁷Institute for Theoretical and Experimental Physics, Moscow, Russia
³⁸Moscow State University, Moscow, Russia
³⁹Institute for High Energy Physics, Protvino, Russia
⁴⁰Petersburg Nuclear Physics Institute, St. Petersburg, Russia
⁴¹Lund University, Lund, Sweden, Royal Institute of Technology and Stockholm University, Stockholm, Sweden, and Uppsala University, Uppsala, Sweden
⁴²Lancaster University, Lancaster, United Kingdom
⁴³Imperial College, London, United Kingdom
⁴⁴University of Manchester, Manchester, United Kingdom
⁴⁵University of Arizona, Tucson, Arizona 85721, USA
⁴⁶Lawrence Berkeley National Laboratory and University of California, Berkeley, California 94720, USA
⁴⁷California State University, Fresno, California 93740, USA
⁴⁸University of California, Riverside, California 92521, USA
⁴⁹Florida State University, Tallahassee, Florida 32306, USA
⁵⁰Fermi National Accelerator Laboratory, Batavia, Illinois 60510, USA
⁵¹University of Illinois at Chicago, Chicago, Illinois 60607, USA
⁵²Northern Illinois University, DeKalb, Illinois 60115, USA
⁵³Northwestern University, Evanston, Illinois 60208, USA
⁵⁴Indiana University, Bloomington, Indiana 47405, USA
⁵⁵University of Notre Dame, Notre Dame, Indiana 46556, USA
⁵⁶Purdue University Calumet, Hammond, Indiana 46323, USA
⁵⁷Iowa State University, Ames, Iowa 50011, USA
⁵⁸University of Kansas, Lawrence, Kansas 66045, USA
⁵⁹Kansas State University, Manhattan, Kansas 66506, USA
⁶⁰Louisiana Tech University, Ruston, Louisiana 71272, USA
⁶¹University of Maryland, College Park, Maryland 20742, USA
⁶²Boston University, Boston, Massachusetts 02215, USA
⁶³Northeastern University, Boston, Massachusetts 02115, USA
⁶⁴University of Michigan, Ann Arbor, Michigan 48109, USA
⁶⁵Michigan State University, East Lansing, Michigan 48824, USA
⁶⁶University of Mississippi, University, Mississippi 38677, USA
⁶⁷University of Nebraska, Lincoln, Nebraska 68588, USA
⁶⁸Princeton University, Princeton, New Jersey 08544, USA
⁶⁹State University of New York, Buffalo, New York 14260, USA
⁷⁰Columbia University, New York, New York 10027, USA
⁷¹University of Rochester, Rochester, New York 14627, USA
⁷²State University of New York, Stony Brook, New York 11794, USA
⁷³Brookhaven National Laboratory, Upton, New York 11973, USA
⁷⁴Langston University, Langston, Oklahoma 73050, USA
⁷⁵University of Oklahoma, Norman, Oklahoma 73019, USA
⁷⁶Oklahoma State University, Stillwater, Oklahoma 74078, USA
⁷⁷Brown University, Providence, Rhode Island 02912, USA
⁷⁸University of Texas, Arlington, Texas 76019, USA
⁷⁹Southern Methodist University, Dallas, Texas 75275, USA
⁸⁰Rice University, Houston, Texas 77005, USA
⁸¹University of Virginia, Charlottesville, Virginia 22901, USA and
⁸²University of Washington, Seattle, Washington 98195, USA

(Dated: March 18, 2008)

We measure the $t\bar{t}$ production cross section in $p\bar{p}$ collisions at $\sqrt{s} = 1.96$ TeV in the lepton+jets channel. Two complementary methods discriminate between signal and background, b -tagging and a kinematic likelihood discriminant. Based on 0.9 fb^{-1} of data collected by the D0 detector at the Fermilab Tevatron Collider, we measure $\sigma_{t\bar{t}} = 7.62 \pm 0.85 \text{ pb}$, assuming the current world average $m_t = 172.6 \text{ GeV}$. We compare our cross section measurement with theory predictions to determine a value for the top quark mass of $170 \pm 7 \text{ GeV}$.

The standard model fixes all properties of the top quark except its mass. The cross section for top quark production depends on the couplings of the top quark and on its mass. In this Letter, we report the most precise measurement of the top-antitop quark pair ($t\bar{t}$) production cross section to date. By comparing the measured cross section to predictions we test whether the top quark conforms with standard model expectations. We also for the first time extract a constraint on the top quark mass based only on this comparison. This determination of the top quark mass is complementary to direct measurements and has the advantage that it is done in a well-defined renormalization scheme, that employed in the calculation of the cross section.

The Tevatron collides protons and antiprotons at $\sqrt{s} = 1.96$ TeV. Most top quarks at the Tevatron are created in pairs through the strong interaction, although evidence of single top quark production has been reported recently [1]. For a top quark mass of 175 GeV, the standard model predicts a $t\bar{t}$ production cross section of about 6.7 pb [2, 3]. Previous measurements [4, 5] agree with this prediction within their precision of 15%. Here we present an substantially improved measurement of the $t\bar{t}$ production cross section, based on data collected by the D0 detector [6] between August 2002 and December 2005 with an integrated luminosity of 0.9 fb^{-1} .

In the standard model the top quark always decays to a W boson and a b quark. The decay modes of the W boson define the possible final states. Here we focus on the lepton+jets channel in which one W boson decays to $e\nu$, $\mu\nu$, or $\tau\nu$ followed by $\tau \rightarrow e\nu\bar{\nu}$ or $\mu\nu\bar{\nu}$. We refer to such leptons as prompt. The other W boson decays to jets or to $\tau\nu$ followed by a hadronic τ decay. The branching fraction for this channel is 38%. The D0 detector acquires these events by triggering on an electron or muon and at least one jet with large momentum component transverse to the beam direction (p_T). The event selection [7] requires exactly one electron or muon, that is isolated from other objects in the detector, with $p_T > 20$ GeV and $|\eta| < 1.1$ (for e) or $|\eta| < 2$ (for μ), missing transverse momentum $\cancel{p}_T > 20$ GeV (for e +jets) or 25 GeV (for μ +jets), and at least three jets with $p_T > 20$ GeV and $|\eta| < 2.5$. The pseudorapidity is defined as $\eta = -\ln|\tan(\theta/2)|$ and θ is the polar angle with the proton beam. The leading jet must have $p_T > 40$ GeV and the lepton p_T and \cancel{p}_T vectors must be separated in azimuth to reject background events with mismeasured particles. Jets are reconstructed using the Run II cone algorithm [8] with cone size $\sqrt{(\Delta\phi)^2 + (\Delta y)^2} = 0.5$, in terms of azimuth ϕ and rapidity y . We call this the inclusive lepton+jets sample. Table I gives the number of selected events (N_{data}). The expected $t\bar{t}$ signal accounts only for about 20% of this sample. Most events origi-

	$e+3 \text{ jets}$	$e+\geq 4 \text{ jets}$	$\mu+3 \text{ jets}$	$\mu+\geq 4 \text{ jets}$
N_{data}	1300	320	1120	306
N_{loose}	2592	618	1389	388
$\epsilon_s(\%)$	84.8 ± 0.3	84.0 ± 1.8	87.3 ± 0.5	84.5 ± 2.2
$\epsilon_b(\%)$	19.5 ± 1.7	19.5 ± 1.7	27.2 ± 5.4	27.2 ± 5.4
$N_{t\bar{t}}$	182 ± 20	156 ± 17	137 ± 15	129 ± 14
$N_{W\text{jets}}$	718 ± 42	69 ± 20	802 ± 26	131 ± 16
N_{other}	132 ± 15	35 ± 4	139 ± 15	36 ± 4
N_{jj}	268 ± 34	60 ± 10	42 ± 14	10 ± 6

TABLE I: Event counts in the inclusive lepton+jets sample.

nate from other processes that produce prompt leptons and jets (mostly W +jets production) and from events with jets which mimic the signature of a lepton. We use two complementary techniques to distinguish the $t\bar{t}$ signal from these backgrounds; b -tagging and a kinematic likelihood discriminant.

We model the $t\bar{t}$ signal and all backgrounds with prompt leptons using Monte Carlo (MC) simulations. We carry out the analyses using $t\bar{t}$ events generated at a reference mass of 175 GeV. W +jets and Z +jets production are generated using the ALPGEN [9] generator and PYTHIA [10] for showering. A matching algorithm [11] avoids double counting of final states. Single top production is generated using SINGLETOP [12] and COMPHEP [13]. Diboson and $t\bar{t}$ production are generated by PYTHIA. All simulated events are processed by a detector simulation based on GEANT [14] and by the same reconstruction programs as the collider data.

We first determine the background from events without prompt leptons in the inclusive lepton+jets sample using loose data samples defined by relaxing the electron identification and the muon isolation requirements. We use simulated events to determine the probability ϵ_s for leptons from W boson decays that satisfy the loose selection to also pass the selection used for the measurement. We correct this efficiency for known differences between efficiencies observed in the MC simulation and in data. We determine the corresponding efficiency ϵ_b for misidentified leptons using data selected with the criteria given above except for requiring $\cancel{p}_T < 10$ GeV to minimize contributions from leptons from W boson decays. The number of events in our selected sample is $N_{\text{data}} = N_{\ell j} + N_{\text{jj}}$, where $N_{\ell j}$ is the number of events with prompt leptons and N_{jj} the number of events without prompt leptons. The number of events in the corresponding loose sample is $N_{\text{loose}} = N_{\ell j}/\epsilon_s + N_{\text{jj}}/\epsilon_b$. These two equations determine N_{jj} given in Table I. We predict the number of events, N_{other} , from the smaller background processes (single top, Z +jets, and diboson production) using the MC simulation and next-to-leading order cross sections [15].

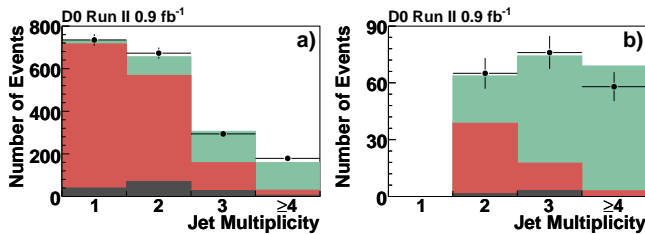


FIG. 1: Jet multiplicity spectra for e +jets and μ +jets events (a) with one b -tagged jet and (b) with at least 2 b -tagged jets. The histogram shows (from top to bottom) the contributions from $t\bar{t}$ production, and from backgrounds with prompt leptons and without prompt leptons.

	3jets,1tag	3jets, ≥ 2 tags	≥ 4 jets,1tag	≥ 4 jets, ≥ 2 tags
$N_{t\bar{t}}$	147 ± 12	57 ± 6	130 ± 10	66 ± 7
$N_{W\text{jets}}$	105 ± 5	10 ± 1	16 ± 2	2 ± 1
N_{other}	27 ± 2	5 ± 1	8 ± 1	2 ± 1
N_{jj}	27 ± 6	3 ± 2	6 ± 3	0 ± 2
total	306 ± 14	74 ± 6	159 ± 11	69 ± 7
N_{data}	294	76	179	58

TABLE II: Numbers of events in the b -tagged analysis.

For the b -tag analysis, we start with the expected $t\bar{t}$ cross section to get a first estimate of the number of $t\bar{t}$ events in the sample. After we obtain a cross section as described below we update this estimate using the measured cross section and iterate the cross section calculation until the result is stable. We fix the number of W +jets events in the inclusive sample so that the sum of all background and signal contributions equals the observed number of events.

The b -tag analysis enhances signal purity by requiring that at least one jet be tagged as a b -jet, i.e., identified to contain the decay of a long-lived particle such as a b -hadron [16]. We determine the number of background events without prompt leptons as above and the number of events expected from other background sources from the number of background events in the inclusive sample times their probability to be b -tagged. We obtain the b -tagging probability from the MC simulation corrected for differences in the b -tagging efficiencies observed in the simulation and in data. In order for the MC model to correctly predict the number of lepton+jets events with two jets with at least one b -tagged jet, we have to scale the number of W +jets events with heavy quarks (b , c) by a factor of 1.17 ± 0.18 relative to the rest of the W +jets events. We use the same scale factor for $W+\geq 3$ jet events. Figure 1 shows the jet multiplicity spectrum of events with b -tags compared to expectations. The composition of the b -tagged samples is given in Table II. The $t\bar{t}$ contribution in Fig. 1 and Tables I and II is based on the cross section measured in the b -tag analysis.

We calculate the cross section using a maximum like-

lihood fit [17] to the number of events in eight different channels defined by lepton flavor (e , μ), jet multiplicity (3, ≥ 4), and b -tag multiplicity (1, ≥ 2). The likelihood is defined as $\mathcal{L} = \prod_i \mathcal{P}(N_i, \mu_i(\sigma_{t\bar{t}}))$, where i runs over the eight channels and $\mathcal{P}(N, \mu)$ is the Poisson probability to observe N events when μ are expected. The expected number of events is the sum of the number of events from all backgrounds plus the number of $t\bar{t}$ events as a function of $\sigma_{t\bar{t}}$. We obtain $\sigma_{t\bar{t}} = 8.05 \pm 0.54(\text{stat}) \pm 0.70(\text{syst}) \pm 0.49(\text{lumi})$ pb for $m_t = 175$ GeV. The third uncertainty arises from the measurement of the integrated luminosity [18].

Table III lists the systematic uncertainties which arise from the following main categories. *Selection* covers acceptance and efficiency for leptons and jets. *Jet energy calibration* accounts for jet energy scale and resolution. The b -tagging efficiencies for b , c , and light quark/gluon jets make up the b -tagging uncertainty. *MC model* uncertainties originate from the cross sections used to normalize the simulated backgrounds, differences observed between $t\bar{t}$ samples generated with ALPGEN and PYTHIA, the factorization and renormalization scale in the W +jets simulation, and the parton distributions functions (PDF). N_{jj} covers the determination of the number of events without prompt leptons.

source	b -tag	likelihood	combined
selection efficiency	0.26 pb	0.25 pb	0.25 pb
jet energy calibration	0.30 pb	0.11 pb	0.20 pb
b -tagging	0.48 pb	—	0.24 pb
MC model	0.29 pb	0.11 pb	0.19 pb
N_{jj}	0.06 pb	0.10 pb	0.07 pb
likelihood fit	—	0.15 pb	0.08 pb

TABLE III: Breakdown of systematic uncertainties.

The likelihood analysis is based on kinematic differences between events with $t\bar{t}$ decays and backgrounds. No single kinematic quantity can separate signal and background effectively. We therefore build a likelihood discriminant from 5-6 variables, listed in Table IV, in each channel. The variables were selected to be well modelled

variable	channel
$\sum_{i=3}^{N_j} p_T(i)$	all
$\sum_{i=1}^{N_j} p_T(i) / \sum_{i=1}^{N_j} p_z(i)$	$e+3$ jets, $e+\geq 4$ jets
$\sum_{i=1}^{N_j} p_T(i) + p_T(e) + \cancel{p}_T$	$e+3$ jets, $e+\geq 4$ jets
ΔR between lepton and jet 1	all
ΔR between jets 1 and 2	$e+\geq 4$ jets, $\mu+\geq 4$ jets
$\Delta\phi$ between lepton and \cancel{p}_T	$\mu+3$ jets, $\mu+\geq 4$ jets
$\Delta\phi$ between jet 1 and \cancel{p}_T	$e+3$ jets, $\mu+3$ jets
sphericity	all but $\mu+3$ jets
aplanarity	all but $\mu+3$ jets

TABLE IV: Variables used for the likelihood discriminant. $\Delta R = \sqrt{(\Delta\phi)^2 + (\Delta\eta)^2}$ and i indexes the list of N_j jets with $p_T > 15$ GeV, ordered in decreasing p_T .

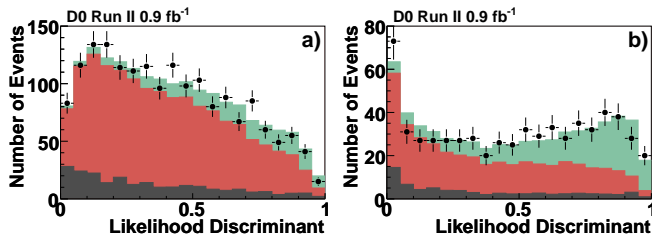


FIG. 2: Likelihood discriminant spectra for e +jets and μ +jets events (a) with 3 jets and (b) with at least 4 jets. See also the caption of Fig. 1.

	3 jets	≥ 4 jets
N_{data}	1760	626
$N_{t\bar{t}}$	245 ± 20	233 ± 19
$N_{W\text{jets}} + N_{\text{other}}$	1294 ± 48	321 ± 30
N_{jj}	227 ± 28	70 ± 12

TABLE V: Sample composition from the likelihood fit.

by the MC simulation and to have good discrimination power. For this analysis, we use the inclusive lepton+jets sample with the additional requirement that events with three jets must satisfy $\sum_{i=1}^{N_j} p_T(i) > 120$ GeV. The events are divided into four channels defined by lepton flavor and jet multiplicity (3, ≥ 4).

We determine the probability density functions of the likelihood discriminant for signal and prompt lepton backgrounds from the simulation and for events without prompt leptons from a control data sample. We perform a maximum likelihood fit to the likelihood discriminant spectra from data in all four channels simultaneously with the $t\bar{t}$ production cross section as a free parameter. The number of events without prompt leptons is constrained to the value obtained from the loose data sample in the same way as described above. Table V gives the sample composition for the best fit and Figure 2 shows the corresponding likelihood discriminant distributions. We measure $\sigma_{t\bar{t}} = 6.62 \pm 0.78(\text{stat}) \pm 0.36(\text{syst}) \pm 0.40(\text{lumi})$ pb for $m_t = 175$ GeV. The systematic uncertainties are listed in Table III in the same categories as for the b -tag analysis plus *Likelihood fit* which gives the uncertainty from statistical fluctuations in the likelihood discriminant shapes from the MC simulation.

We combine the two analyses using the BLUE method [19]. Their statistical correlation factor is 0.31, determined by MC generated pseudodata sets that model the statistical correlation between the two analyses. The systematic uncertainties from each source are completely correlated between both analyses. The combined result is $\sigma_{t\bar{t}} = 7.42 \pm 0.53(\text{stat}) \pm 0.46(\text{syst}) \pm 0.45(\text{lumi})$ pb for $m_t = 175$ GeV with $\chi^2 = 2$ for one degree of freedom, corresponding to a p-value of 0.16. We use samples of $t\bar{t}$ events simulated with different values of the top quark mass to determine the cross section as a func-

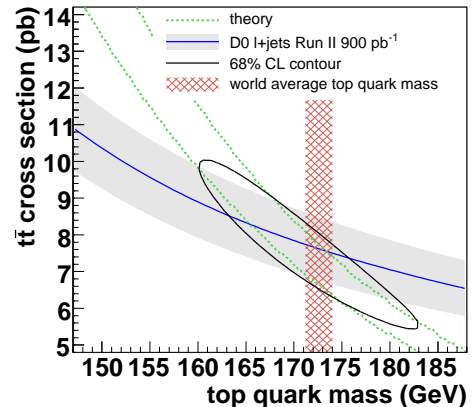


FIG. 3: Comparison of measured cross section and theory prediction versus top quark mass.

tion of top quark mass. A polynomial fit gives $\sigma_{t\bar{t}}/\text{pb} = 7.42 - 7.9 \times 10^{-2} \Delta m + 9.7 \times 10^{-4} (\Delta m)^2 - 1.7 \times 10^{-5} (\Delta m)^3$, where $\Delta m = m_t/\text{GeV} - 175$, as shown in Figure 3.

We define likelihoods as a function of $\sigma_{t\bar{t}}$ and m_t for the theory prediction and our measurement. There are two sources of uncertainty in the calculated cross sections, a theory uncertainty that arises from the termination of the perturbative calculation and the uncertainty from the PDFs. For each value of m_t , we represent the former by a likelihood function that is constant within the ranges given in Refs. [2, 3] and zero elsewhere and the latter by a Gaussian likelihood function with rms equal to the uncertainty determined in Ref. [2] for the CTEQ6M [20] error PDF sets. We then convolute the two functions and average the likelihood functions from the two calculations. The cross section measurement is represented by a Gaussian likelihood function centered on the measured value with rms equal to the total experimental uncertainty. We multiply the theory and measurement likelihoods to obtain a joint likelihood. The contour in Figure 3 shows the smallest region of the joint likelihood that contains 68% of its integral. We integrate over the cross section to get a likelihood function that depends only on the top quark mass. We find that at 68% C.L. $m_t = 170 \pm 7$ GeV, in agreement with the current world average of direct measurements of the top quark mass of 172.6 ± 1.4 GeV [21].

In conclusion, we find that $t\bar{t}$ production in $p\bar{p}$ collisions agrees with standard model predictions. At the world average of direct top quark mass measurements of 172.6 GeV we measure $\sigma_{t\bar{t}} = 7.62 \pm 0.85$ pb. This is the most precise measurement of the $t\bar{t}$ production cross section. By comparing the cross section measurement with the theory prediction we determine the top quark mass to be 170 ± 7 GeV.

We thank the staffs at Fermilab and collaborating institutions, and acknowledge support from the DOE

and NSF (USA); CEA and CNRS/IN2P3 (France); FASI, Rosatom and RFBR (Russia); CNPq, FAPERJ, FAPESP and FUNDUNESP (Brazil); DAE and DST (India); Colciencias (Colombia); CONACyT (Mexico); KRF and KOSEF (Korea); CONICET and UBACyT (Argentina); FOM (The Netherlands); STFC (United Kingdom); MSMT and GACR (Czech Republic); CRC Program, CFI, NSERC and WestGrid Project (Canada); BMBF and DFG (Germany); SFI (Ireland); The Swedish Research Council (Sweden); CAS and CNSF (China); and the Alexander von Humboldt Foundation.

-
- [a] Visitor from Augustana College, Sioux Falls, SD, USA.
 [b] Visitor from The University of Liverpool, Liverpool, UK.
 [c] Visitor from ICN-UNAM, Mexico City, Mexico.
 [d] Visitor from II. Physikalisches Institut, Georg-August-University, Göttingen, Germany.
 [e] Visitor from Helsinki Institute of Physics, Helsinki, Finland.
 [f] Visitor from Universität Zürich, Zürich, Switzerland.
 [‡] Deceased.
- [1] D0 Collaboration, V.M. Abazov *et al.*, Phys. Rev. Lett. **98**, 181802 (2007).
 [2] M. Cacciari *et al.*, JHEP **404**, 068 (2004).
 [3] N. Kidonakis and R. Vogt, Phys. Rev. D **68**, 114014 (2003).

- [4] D0 Collaboration, V.M. Abazov *et al.*, Phys. Rev. D **74**, 112004 (2006); Phys. Rev. D **76**, 052006 (2007).
 [5] CDF Collaboration, A. Abulencia *et al.*, Phys. Rev. Lett. **97**, 082004 (2006).
 [6] D0 Collaboration, V.M. Abazov *et al.*, Nucl. Instrum. Methods Phys. Res., Sect. A **565**, 463 (2006).
 [7] D0 Collaboration, V.M. Abazov *et al.*, Phys. Rev. D **76**, 092007 (2007).
 [8] G. Blazey *et al.*, arXiv:hep-ex/0005012 (2000).
 [9] M.L. Mangano *et al.*, JHEP **307**, 001 (2003).
 [10] T. Sjöstrand *et al.*, arXiv:hep-ph/0308153 (2003).
 [11] S. Höche *et al.*, arXiv:hep-ph/0602031 (2004).
 [12] E.E. Boos *et al.*, Phys. Atom. Nucl. **69**, 1317 (2006).
 [13] E.E. Boos *et al.* (CompHEP Collaboration), Nucl. Instrum. Methods Phys. Res., Sect. A **534**, 250 (2004).
 [14] R. Brun and F. Carminati, CERN Program Library Long Writeup W5013 (1993).
 [15] E.E. Boos *et al.*, Phys. Atom. Nucl. **69**, 1317 (2006); Z. Sullivan, Phys. Rev. D **70**, 114012 (2004); J.M. Campbell and R.K. Ellis, Phys. Rev. D **60**, 113006 (1999).
 [16] T. Scanlon, Ph.D. thesis, FERMILAB-THESIS-2006-43.
 [17] D0 Collaboration, V.M. Abazov *et al.*, Phys. Rev. D **74**, 112004 (2006).
 [18] T. Andeen *et al.*, FERMILAB-TM-2365 (2007).
 [19] L. Lyons, D. Gibaut and P. Clifford, Nucl. Instrum. Methods Phys. Res., Sect. A **270**, 110 (1988); A. Valassi, Nucl. Instrum. Methods Phys. Res., Sect. A **500**, 391 (2003).
 [20] D. Stump *et al.*, J. High Energy Phys. 10 (2003) 046.
 [21] CDF and D0 Collaborations, FERMILAB-TM-2403-E.